International Archive of Applied Sciences and Technology, Vol 1 [2] December 2010: 37 - 43

© Society of Education, India
ISSN 0976- 4828
http:// www.soeagra.com

RESEARCH ARTICLE

Comparison of Low Field Electron Transport Characteristics in InP, GaP and $Ga_{0.52}In_{0.48}P$ Crystal Structures

[1]H. Arabshahi and [2]G. R. Ebrahimi
[1]Department of Physics, Ferdowsi University of Mashhad, Mashhad, Iran
[2]Department of Metalogy, Sabzevar Tarbiat Moallem University, Sabzevar, Iran
Email: g.rebrahimi@yahoo.com

ABSTRACT
Temperature and doping dependencies of electron mobility in InP, GaP and $Ga_{0.52}In_{0.48}P$ structures have been calculated using an iteravive technique. The following scattering mechanisims, i.e, impurity, polar optical phonon, acoustic phonon and piezoelectric are inculded in the calculation. Ionized imurity scattering has been treated beyound the Born approximation using the phase-shift analysis. It is found that the electron mobility decreases monotonically as the temperature increases from 100K to 500K for each material which is depended to their band structures characteristics. The low temperature value of electron mobilty increases significantly with increasing doping concentration. The iterative results are in fair agreement with other recent calculations obtained using the relaxation-time approximation and experimental methods.
***KEYWORDS**: Iteravive technique; Ionized imurity scattering; Born approximation; electron mobility.*

INTRODUCTION

The ternary semiconductor, $Ga_{0.52}In_{0.48}P$ offers a large direct band gap of the III-V compound semiconductor material which is lattice matched to a commonly available substrate like GaP or InP. Owing to its relatively large band gap, this material has been cited for its potential use in visible light emitters such as light emitting diodes and lasers [1-4]. $Ga_{0.52}In_{0.48}P$ has further potential usage as a visible light detector as well as in high temperature and/or high power electronics. The additional advantage of being lattice matched to the binary compound GaP, InP as well as GaAs offers large flexibility in the choice of heterostructures which can be made from this material. To date, a GaInP/AlGaInP double heterostructure laser grown on a GaAs substrate has been successfully demonstrated at room-temperature cw operation [5]. Improved electron transport properties are one of the main targets in the ongoing study of binary and ternary and GaP, InP and $Ga_{0.52}In_{0.48}P$ materials. The iterative technique has proved valuable for studying non-equilirium carrier transport in arange of semiconductor materials and devices [6-7]. However, carrier transport modeling of $Ga_{0.52}In_{0.48}P$ materials has only recently begun to receive sustained attention, now that the growth of compounds and alloys is able to produce valuable material for the electronics industry. In this communication we present iterative calculations of electron drift mobility in low electric field application. We demonstrate the effect of low electric field on the electron transport properties in these materials. The differences in transport properties are analyzed in terms of important material parameters. Most of the calculations have been carried out using a non-parabolic ellipsoidal valley model to describe transport in the conduction band. However, the simpler and less computationally intensive spherical parabolic band scheme has also been applied, to test the validity of this approximation. The iterative calculations take into account the electron-lattice interaction through polar optical phonon scattering, deformation potential acoustic phonon scattering (treated as an elastic process) and piezoelectric scattering. Impurity scattering due to ionized and neutral donors is also included, with the latter found to be important at low temperature due to the relatively large donor binding energy which implies considerable carrier freeze-out already at liquid nitrogen tempearure.

This paper is organised as follows. Details of the iterative model and the electron mobility calculations are presented in section II, the electron scattering mechanism which have been used are discussed in section III and the results of iterative calculations carried out on GaP, InP and $Ga_{0.52}In_{0.48}P$ materials are interpreted in section IV.

SIMULATION METHOD

In principle the iterative technique give exact numerical prediction of electron mobility in bulk semiconductors. To calculate mobility, we have to solve the Boltzmann equation to get the modified probability distribution function under the action of a steady electric field. Here, we have adopted the iterative technique for solving the Boltzmann transport equation. Under application of a uniform electric field the Boltzmann equation can be written as

$$(\frac{e}{\hbar})E.\nabla_k f = \oint [s' f'(1-f) - sf(1-f')]dk \qquad (1)$$

where $f = f(k)$ and $f' = f(k')$ are the probability distribution functions and $s = s(k,k')$ and $s' = s(k',k)$ are the differential scattering rates. If the electric field is small, we can treat the change from the equilibrium distribution function as a perturbation which is first order in the electric field. The distribution in the presence of a sufficiently small field can be written quite generally as

$$f(k) = f_0(k) + g(k)\cos\theta \qquad (2)$$

where $f_0(k)$ is the equilibrium distribution function, θ is the angle between k and E and $g(k)$ is an isotropic function of k, which is proportional to the magnitude of the electric field. In general, contributions to the differential scattering rates come from two types of scattering processes, elastic scattering s_{el}, due to acoustic, impurity, plasmon and piezoelectric phonons, and inelastic scattering s_{inel}, due to polar optic phonons

$$s(k,k') = s_{el}(k,k') + s_{inel}(k,k') \qquad (3)$$

Generally this scattering process can not be treated within the framework of the relaxation time approximation because of the possibility of the significant energy exchange between the electron and the polar optic modes. In this case, s_{inel} represents transitions from the state characterized by k to k' either by emission $[s_{em}(k,k')]$ or by absorption $[s_{ab}(k,k')]$ of a phonon. The total elastic scattering rate will be the sum of all the different scattering rates which are considered as elastic processes, i.e. acoustic, piezoelectric, ionized impurity, and electron-plasmon scattering. In the case of polar optic phonon scattering, we have to consider scattering-in rates by phonon emission and absorption as well as scattering-out rates by phonon absorption and emission. Using Boltzmann equation and considering all differential scattering rates, the factor $g(k)$ in the perturbed part of the distribution function $f(k)$ can be given by

$$g(k) = \frac{\frac{-eE}{\hbar}\frac{\partial f_0}{\partial k} + \sum\int g'\cos\varphi[s_{inel}'(1-f) + s_{inel} f)]dk}{\sum\int(1-\cos\varphi)s_{el}\,dk + \sum\int[s_{inel}(1-f') + s_{inel}' f']dk} \qquad (4)$$

Note, the first term in the denominator is simply the momentum relaxation rate for elastic scattering. It is interesting to note that if the initial distribution is chosen to be the equilibrium distribution, for which $g(k)$ is equal zero, we get the relaxation time approximation result after the first iteration. We have found that convergence can normally be achieved after only a few iterations for small electric fields. Once $g(k)$ has been evaluated to the required accuracy, it is possible to calculate quantities such as the drift mobility which is given by

$$\mu_d = \frac{\hbar}{3m}\frac{\int_0^\infty k^3 \frac{g(k)}{Ed}dk}{\int_0^\infty k^2 f(k)dk} \qquad (5)$$

Where d is defined as $1/d = m\nabla_k E/\hbar^2 k$. In the following section electron-phonon, electron impurity and electron-plasmon scattering mechanisms will be discussed.

ELECTRON SCATTERING MECHANISMS

A. Phonon scattering

The dominant scattering mechanism of electrons in polar semiconductors like GaP, InP and $Ga_{0.52}In_{0.48}P$ comes from the electron-phonon interaction except at the lowest temperatures. The electron-optical phonon interaction contributes both in the ohmic and non-ohmic mobility and provides the dominant energy-loss mechanism of electrons. First order polarization occurs in connection with the primitive unit cell, characteristic of the longitudinally polarized optical mode. In thesematerials the Debye temperature is more than 800K [6], hence polar optical phonon scattering must be considered as an inelastic process. Other phonon scattering processes, i.e. acoustic and piezoelectric scattering are considered as elastic processes. Like GaAs; GaP, InP and $Ga_{0.52}In_{0.48}P$ also has a single minimum valley at K= 0 (Γ valley). So internally phonon scattering can be neglected at low field conditions. In polar optic phonon scattering the differential scattering rates for absorption and emission can be written as [5]

$$S_{op}(k,k') = \frac{\sqrt{2m^*}e^2\omega_{op}}{8\pi\varepsilon_0\hbar}\left(\frac{1}{\varepsilon_\infty}-\frac{1}{\varepsilon_s}\right) \frac{1+2\alpha E'}{\gamma^{1/2}(E)} F_0(E,E')\left\{N_{op},(N_{op}+1)\right\} \quad (6)$$

where ε_s and ε_∞ are define in table 1, N_{op} is the phonon occupation number and the N_{op} and $1+N_{op}$ refer to absorption and emission, respectively. For small electric fields, the phonon population will be very close to equilibrium, so that the average number of phonons is given by the Bose-Einstein distribution function. We have found that after a few iterations, the electron polar optical phonon scattering rate converges and becomes very close to the experimental result [6]. The energy range involved in the case of scattering by acoustic phonons is from 0 to $2\hbar v_s k$, as the momentum conservation restricts the phonon wave vector q between 0 and 2k , where k is the electron wave vector. Typically the average value of k is on the order of 10^7 cm^{-1} and v_s, the velocity of sound in the medium, is on the order of 10^5 cm/s. Hence, $2\hbar v_s k \approx 1$ meV, which is small compared to the thermal energy. Hence electron-acoustic phonon scattering can be considered as an elastic process. Actually, a long wave length acoustic displacement can not affect the energy since neighboring unit cells move by almost the same amount, only the differential displacement (normally the strain) is of importance. The total differential scattering rate for acoustic phonons can be given by

$$S_{ac}(k,k') = \frac{\sqrt{2}D_{ac}^2(m_t^* m_l^*)^{1/2}K_B T}{\pi\rho v^2\hbar^4} \frac{\sqrt{E(1+\alpha E)}}{(1+2\alpha E)}\left[(1+\alpha E)^2+1/3(\alpha E)^2\right] \quad (7)$$

where D_{ac} is the acoustic deformation potential, ρ is the material density and α is the non-parabolicity coefficient. The formula clearly shows that the acoustic scattering increases with temperature.

In crystals like GaP, whose lattice lacks inversion symetry, such as those semiconductors with sphacelate or wurtzite structure, elastic strain may be accompanied by macroscopic electric fields. This piezoelectric effect provides an additional coupling between the electric and acoustic vibrations. The differential scattering rate for piezoelectric scattering will be

$$S_{pz}(k,k') = \frac{\sqrt{m^*}e^2K_{ac}^2K_B T}{4\sqrt{2}\pi\varepsilon_0\varepsilon_s\hbar^2}\gamma^{-1/2}(E) (1+2\alpha E)^2\times Ln\left(1+\frac{8m^*\gamma(E)}{\hbar^2 q_0^2}\right) \quad (8)$$

where K_{av} is the dimensionless so called average electromechanical coupling constant [7].

B. Impurity scattering

The standard technique for dealing with ionized impurity scattering in semiconductors is the Brook-Herring (BH) technique [8], which is based on two inherent approximations. First, is the first order Born approximation and second is the single ion screening approximation. These two approximations essentially lead to a poor fit to the experimental mobility data [9,10]. Several attempts have been

made to modify the BH technique phenomenologically [11]. It has been shown that phase-shift analysis of electron-impurity scattering is the best way to overcome the Born approximation. Departure from the BH prediction of electron mobility is evident at higher electron concentrations. Meyer and Bartoli [9] have provided an analytic treatment based on phase-shift analysis taking into account the multi-ion screening effect and finally been able to overcome both the approximations. All the previous techniques of impurity screening by free electrons in semiconductors were based on the Thomas-Fermi (TF) approximation which assures that a given impurity should be fully screened. The breakdown of the single-ion screening formalism becomes prominent in the strong screening regime, where the screening length calculated through TF theory becomes much shorter than the average distance between the impurities and hence neighboring potentials do not overlap significantly. This essentially leads to a physically unreasonable result. In the case of high compensation, the single-ion screening formalism becomes less relevant, because in order to maintain the charge neutrality condition, it would be more difficult for a given number of electrons to screen all the ionized donors separately. In the case of InP, the compensation ratio is usually quite large, and the ratio N_D^+/n is also temperature dependent. Hence the multi-ion screening correction is very essential in InP. The effective potential of an ionized impurity scattering center is spherically symmetric in nature, so one can use phase-shift analysis to find the differential scattering rate $s(k,k')$ more accurately. The effective potential $V(r)$ due to an ionized impurity can be expressed as $V(r)=-(Z_i e^2)/(4\pi\varepsilon_0\kappa_0 r)e^{-r/\lambda}$, where Z_i is the charge of the ionized impurity in units of e and λ is the screening length. The standard technique to find out the screening length is the TF approach which is based on single ion screening approximation. In TF one can calculate the charge contribution q_i to the screening of a single ionized donor by an electron of energy E_i and is given by $q_i=-(2e^3\lambda^2/\varepsilon_0\kappa_0 E_i V)$. In the case of multi-ion problem, the TF approach can be generalized to find out the effective charge contribution due to an electron to screen all ionized donors and can be given by $Q_i=-(2e^3 N_D^+\lambda^2/\varepsilon_0\kappa_0 E_i)$. Total screening charge exactly neutralizes the ionized donors, when Q_i is summed over all electronic states

$$\sum_i -\frac{Q_i}{e} f_0(E_i) = N_D^+ \tag{9}$$

For the sufficiently low energy electrons, Q_i can be greater than the electronic charge, which is physically unreasonable. One way to tackle [9] this problem is to introduce a factor S_i such that

$$S_i(E_i)=\frac{E_i}{\xi} \tag{10}$$

where $\xi=(2N_D^+c^2\lambda^2/\varepsilon_0 k_0)$, Q_i will be modified to $Q_i'=Q_i S_i$ in Eq. (9). For the low energy electrons the contribution will be –e. Since the total contribution to the screening by the low energy electrons has been effectively decreased, Eq. (9) no longer holds. However, if the screening length λ is more than the average distance between the donors, it is not necessary to insist that each donor be fully screened, only it is required that overall charge neutrality should be preserved. Electrons in the overlap region can provide screening to both the ionized donors. Here we can define a factor p, which would be the fraction of the total charge, which is contained within a sphere of radius R surrounding the donor. Hence Eq. (9) will be modified as

$$\sum_i -\frac{Q_i''}{e} f_0(E_i)=pN_D^+ \tag{11}$$

where $Q_i''=pQ_iS_i$. The screening charge requirement will be fulfilled by adjusting the creening length untill Eq. (11) is satisfied and is given by

$$\lambda_m^{-2}=\eta\lambda_0^{-2} \tag{12}$$

where λ_m is multi-ion screening length and λ_0 is TF screening length. The differential scattering rate for ionized impurity can be given as

$$S_{ii}(k,k')=\frac{8\pi^3\hbar^3}{m^{*2}V^2}\left|f(X)\right|^2\delta[E(k')-E(k)] \tag{13}$$

where scattering amplitude $f(X)$ depends on the phase shift δ_l and Legendre polynomial P_l and is given by

$$f(X) = \frac{1}{2ik}\sum_{l=0}^{\infty}(2l+1)(e^{2i\delta_l}-1)P_l(X) \qquad (14)$$

It has already been mentioned that in n-type GaP the activation energy of the donors is quite large, which keeps a large number of donors neutral at low temperatures. Neutral impurity scattering has been dealt with previously using the Erginsoy [12] expression which is based on electron scattering by a hydrogen atom and a scaling of the material parameters. It has been shown that an error as high as 45% results in the neutral impurity scattering cross section with this simple model. Meyer and Bartoli [9] have given a phase shift analysis treatment based on the variation results of Schwartz [13] to calculate the neutral impurity cross section, which is applicable for a larger range of electron energy.

III- Calculation results

We have performed a series of low-field electron mobility calculations for GaP, InP and $Ga_{0.52}In_{0.48}P$ materials. Low-field mobilities have been derived using iteration methode.
Figure 1 shows the calculated electron drift mobility in bulk GaP, InP and $Ga_{0.52}In_{0.48}P$ materials as a function of temperature with free electron concentration of 10^{22} m^{-3} and with the electric field applied along one of the cubic axes. It can be seen from the figure that the electron drift mobilities at room temperature that we find for GaP is 2500 cm^2/V-s while those for $Ga_{0.52}In_{0.48}P$ and InP are about 11000 and 13000 cm^2/V-s, respectively, for an electric field equal to 10^4 Vm^{-1}. The results plotted in figure 1 indicate that the electron drift mobility of GaP is lower than other structure at all temperatures. This is largely due to the higher Γ valley effective mass in the GaP phase. Also it can be seen that below 100 K, ionized impurity and piezoelectric scattering are the dominant forms of lattice scattering. The approximate $T^{-1/2}$ mobility dependence near 100 K signals the dominance of ionized impurity and piezoelectric scattering.

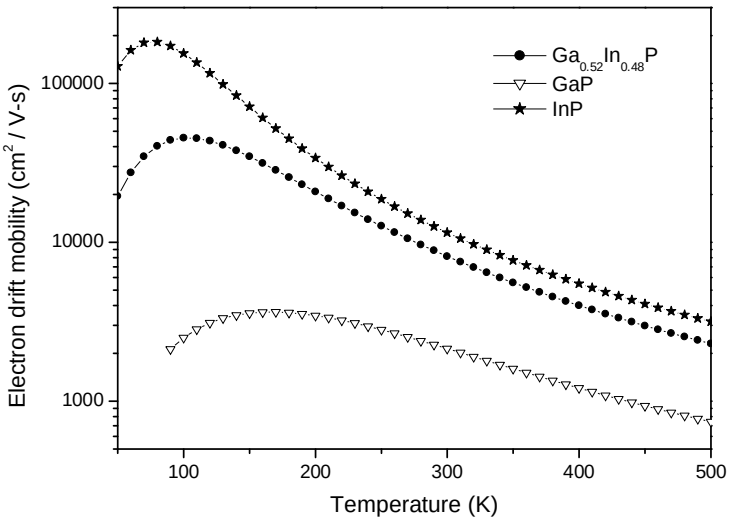

Fig 1. Electron drift mobility vs temperature of pure intrinsic GaP, InP and $Ga_{0.52}In_{0.48}P$ Impurity and piezoelectric scattering dominate the data below 100 K.

Figure 2 shows the calculated variation of the electron drift mobility as a function of free electron concentration for all crystal structures at room temperature. The mobility does not vary monotonically between free electron concentrations of 10^{20} m^{-3} and 10^{24} m^{-3} due to the dependence of electron scattering on free electron concentration, but shows a maximum near 10^{20} m^{-3} for all structures.

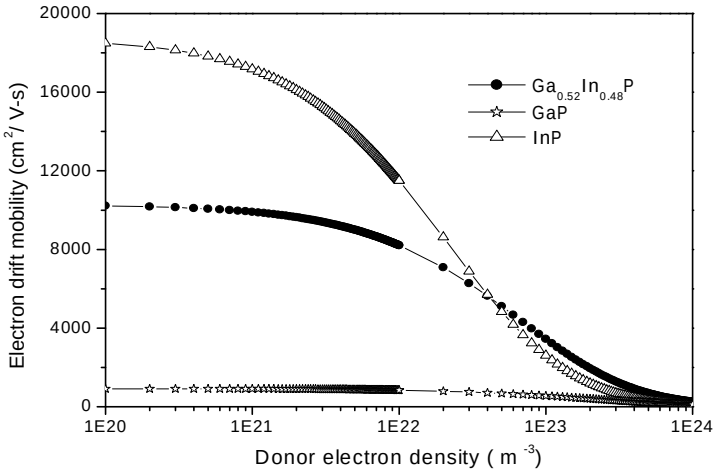

Fig 2. Calculated low-field electron drift mobility of GaP, InP and $Ga_{0.52}In_{0.48}P$ as a function of different free electron concentration at room temperature.

In figure 3, the electron density as a function of temperature using the screened shallow donor binding energy have been calculated for different background electron concentrations. The temperature effects on the carrier screening are taken into account for this calculation. The figure clearly shows that for uncompensated GaP, InP and $Ga_{0.52}In_{0.48}P$ at liquid nitrogen temperature there is a large fraction of neutral donor impurities present.

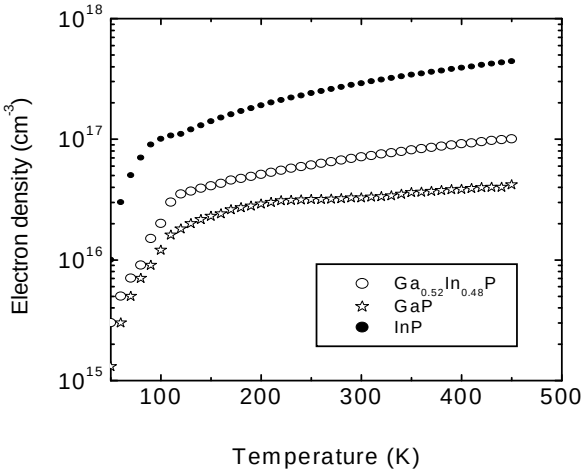

Fig.3. Electron concentration versus temperature for GaP, InP and $Ga_{0.52}In_{0.48}P$ with different donor doping densities.

The variation of the electron drift mobility in $Ga_{0.52}In_{0.48}P$ with temperature for various types of scattering mechanisms such as ionized impurity, acoustic phonon via deformation potential, piezoelectric scattering and polar optical phonon scattering individually.

It is evident from this figure that at very high temperatures the mobility is limited by longitudinal optical phonon scattering, whereas the mobility varies inversely with donor concentration at low temperature, as we would expect from the foregoing discussion. The decrease in mobility at low temperature is caused in part by neutral impurity scattering. For the lowest doping concentration considered in this calculation, 10^{21} cm^{-3}, we find that the neutral impurity scattering plays a large role at low temperature because of the significant carrier freeze-out evident from figure 3.

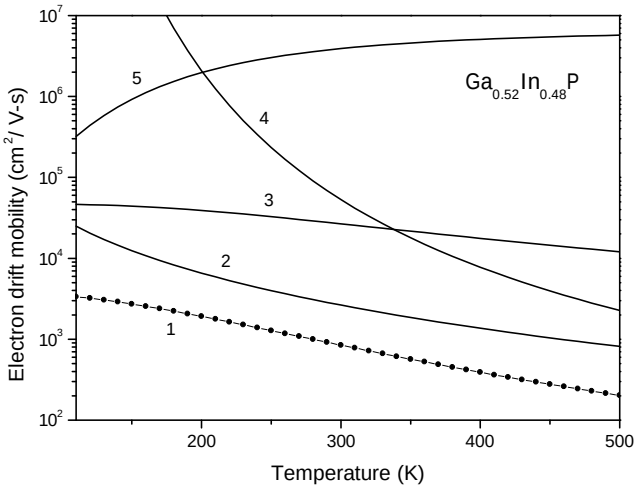

Fig.4. Electron drift mobility versus temperature in $Ga_{0.52}In_{0.48}P$ for acoustic phonons via deformation potential (3), piezoelectric (2), ionized impurity (4), polar optical phonon (5) and with including all scattering processes (1).

CONCLUSION

In conclusion, we have quantitatively obtained temperature-dependent and electron concentration-dependent electron mobility in GaP, InP and $Ga_{0.52}In_{0.48}P$ materials using an iteravive technique. The theoretical values show good agreement with recently obtained experimental data. It has been found that the low-field mobility is significantly higher for the InP due to the higher electron effective mass in this structure. Several scattering mechanisms have been included in the calculation. Ionized impurities have been treated beyond the Born approximation using a phase shift analysis. Screening of ionized impurities has been treated more realistically using a multi-ion screening formalism, which is more relevant in the case of highly compensated III-V semiconductors like GaAs.

ACKNOWLEDGEMENTS

I would like to thank Maryam Gholvani for writing up the paper.

REFERENCES

[1] S Nakamura, M Senoh and T Mukai, Appl. Phys. Lett. **62**, 2390 (1993).
[2] S Strite and H Morkoc, J. Vac. Sci. Technol. **B 10**, 1237 (1992).
[3] V W L Chin and T L Tansley, J. Appl. Phys. **75**, 7365 (1994).
[4] D L Rode and D K Gaskill, Appl. Phys. Lett. **66**, 1972 (1995).
[5] C Moglestue, *Monte Carlo simulation of semiconductor devices*, Chapman and Hall (1993).
[6] K T Tsen, D K Ferry, A Botchkarev, B Suerd, A Salvador and H Morkoc, Appl. Phys. Lett. **71**, 1852 (1997).
[7] B K Ridley, Electrons and phonons in semiconductor multilayers, Cambridge University press (1997).
[8] H Brooks, Phys. Rev. **83**, 879 (1951).
[9] J R Meyer and F J Bartoli, Phys. Rev. **B 23**, 5413 (1981).
[10] J R Meyer and F J Bartoli , *Solid State State* Commun. **41**, 19 (1982).
[11] D Chattopadhya and H J Queisser, *Rev. Mod. Phys.* **53**, 745 (1981).
[12] C Erginsoy, Phys. Rev. **79**, 1013 (1950)
[13] C Schwartz, Phys. Rev. **124**, 1468 (1961)
[14] M V Fischetti, Phys. Rev. **44**, 5527 (1991)
[15] H Morkoc, *Nitride semiconductor and devices*, Springer-velag (1999)
[16] Udayan, V Bhapkar and M S Shur, J. Appl. Phys. **82**,1649 (1997)
[17] R P Wang, P P Ruden, J Kolnik and K F Brennan, *Mat. Res. Soc. Symp. Proc.*, **445**, 935 (1997)